

MONITORING INJECTION PRESSURE DATA TO PREDICT PERFORMANCE OF
ACID FRACTURING JOBS IN HORIZONTAL WELLS

A Thesis

by

TALAL SAAD M AL SHAFLOOT

Submitted to the Office of Graduate and Professional Studies of
Texas A&M University
in partial fulfillment of the requirements for the degree of

MASTER OF SCIENCE

Chair of Committee,	Ding Zhu
Committee Members,	A. Daniel Hill
	Marcelo Sanchez
Head of Department,	A. Daniel Hill

August 2016

Major Subject: Petroleum Engineering

Copyright 2016 Talal Al Shafloot

ABSTRACT

Evaluating the success of an acid fracturing job using injection pressure data is a valuable tool to diagnose the success of the treatment. In this work, a new strategy of analyzing the performance of acid fracturing jobs is presented. The strategy includes analyzing different plots of injection pressure data simultaneously to understand the progress of the job and identify some fracture parameters.

The new strategy can evaluate four main aspects of an acid treatment: the propagation and evolution of the fracture, the general shape of the fracture, fracture area and the type of treatment undergoing either etching or matrix acidizing. Combining different studies to analyze the trends of Δp on log-log plot to make conclusions is one of the main scopes of the study. A new approach in this work is applied to predict the area of fracture by adjusting the transient dual porosity solutions used for production data to accommodate the conditions of acid fracturing. The new technique allows use of modified models to interpret bilinear flow regimes and determine the fracture area.

This strategy has been applied to three horizontal fractured wells. The proposed technique was used to understand the fracture status at different stages during the treatment. The fracture area was calculated at different periods, showing the signature of bilinear flow with a quarter slope on the log-log plot of Δp vs. time. Calculated fracture area was compared to the one obtained from production data, and the results showed similarity.

The novelty of the new strategy is that it evaluates the performance of acid fracturing jobs without the need of either mechanical properties of the rock or production data. In addition, this strategy can be adapted for hydraulic fracturing treatments.

DEDICATION

To my family and my uncle Abdullah Al-Abood

ACKNOWLEDGEMENTS

I would like to thank my adviser Dr. Zhu for her support, guidance and kindness. I would like also to thank Dr. Hill and Dr. Sanchez for the support and serving as committee members.

Thanks also go to my friends and colleagues in the University for making my time at Texas A&M University a great experience. I want to extend my gratitude to King Fahd University of Petroleum and Minerals for the sponsorship and support throughout my Master's degree.

Finally, I thank my mother, father, brothers and sisters for their encouragement, support, patience and love.

NOMENCLATURE

- A_{cm} = total matrix surface area draining into fracture system, ft²
 c_t = total compressibility, M⁻¹L⁻¹T², psi⁻¹
 h = reservoir thickness, ft.
 k = permeability, L², md
 k_f = bulk fracture permeability of dual porosity models, md
 k_m = matrix permeability, md
 L = general fracture spacing, ft.
 m = slope of linear function between flow rate, pressure and time
 \tilde{m}_4 = slope of regions 4 (matrix linear flow region)
 $m(p)$ = pseudopressure (gas), psi⁻²/cp
 m_D = dimensionless psuedo pressure
 m_{DL} = dimensionless pressure (rectangular geometry, gas)
 p = pressure drop, ML⁻¹T⁻², psi
 p_D = dimensionless pressure, dimensionless
 p_{DL} = dimensionless pressure based on Ac^{0.5} (rectangular geometry, liquid, dual porosity)
 p_i = initial reservoir pressure, ML⁻¹T⁻², psi
 p_{wf} = bottom flowing pressure, ML⁻¹T⁻², psi
 q_g = gas rate, Mscf/day
 q_w = flow rate in the wellbore, L³t⁻¹, bbl/min
 t = time, hours
 T = absolute temperature, °R
 t_D = dimensionless time
 t_{DAc} = dimensionless time based on Ac (rectangular geometry, dual porosity)
 u = Laplace space variable
 w = fracture width, ft
 x_f = fracture-half length, ft.
 y_e = drainage area half-width (rectangular geometry), ft

Z = gas compressibility factor

Greek

Δp_f	=	frictional pressure drop, $ML^{-1}T^{-2}$, psi
Δp_{PE}	=	hydrostatic pressure drop, $ML^{-1}T^{-2}$, psi
Δt_{sup}	=	superposition time function
λ_{Ac}	=	dimensionless interporosity parameter
μ	=	viscosity, $ML^{-1}T^{-1}$, cp
ρ	=	density, ML^{-3} , g/cm^3
ϕ	=	porosity, fraction
ω	=	dimensionless storativity ratio

Subscripts

i	=	Initial
f	=	Fracture
m	=	Matrix
$f+m$	=	total system (fracture + matrix)
sc	=	standard condition
sf	=	surface

TABLE OF CONTENTS

	Page
ABSTRACT	ii
DEDICATION.....	iv
ACKNOWLEDGEMENTS	v
NOMENCLATURE	vi
TABLE OF CONTENTS	viii
LIST OF FIGURES	x
LIST OF TABLES.....	xi
CHAPTER I INTRODUCTION AND LITERATURE REVIEW.....	1
Introduction.....	1
Literature review	4
Research objectives	8
CHAPTER II DEVELOPMENT OF THE METHODOLOGY.....	9
Monitoring injection pressure	9
Proposed methodology	24
Production data	33
CHAPTER III RESULTS AND DISCUSSION	34
Well A	34
Well B.....	40
Well C.....	45
Discussion.....	49
Limitations of the proposed methodology	53
CHAPTER IV CONCLUSIONS AND RECOMMENDATIONS.....	55
Conclusions.....	55
Recommendations	56

REFERENCES	57
------------------	----

LIST OF FIGURES

	Page
Figure 1.1: Role of etching in maintaining fracture width (Kalfayan, 2007).....	2
Figure 2.1: PKN fracture geometry (Geertsma et al., 1969).....	11
Figure 2.2: KGD fracture geometry (Geertsma et al., 1969)	12
Figure 2.3: Initiation and propagation of different models (Nolte, 1991)	13
Figure 2.4: Interpretations of different slopes of P_{net} plots (Nolte, 1988)	15
Figure 2.5: Khristianovich fracture (Conway et al., 1985)	17
Figure 2.6: Perkins and Kern fracture (Conway et al., 1985)	17
Figure 2.7: Penny fracture (Conway et al., 1985)	18
Figure 3.1: Pressure above closure - Well A.....	35
Figure 3.2: Inverse injectivity plot - Well A	37
Figure 3.3: Combined plots analysis - Well A	38
Figure 3.4: Production history for Well A	39
Figure 3.5: Normalized pseudo pressure plot - Well A	40
Figure 3.6: Pressure above closure plot - Well B	42
Figure 3.7: Inverse injectivity plot - Well B	43
Figure 3.8: Combined plot - Well B	44
Figure 3.9: Production history for Well B	45
Figure 3.10: Downhole flowing pressure analysis - Well C	47
Figure 3.11: Combined plots – Well C	48

LIST OF TABLES

	Page
Table 2.1: Interpretation of slopes in pressure above closure plot	26
Table 3.1: Reservoir and fracture parameters for Well A.....	34
Table 3.2: Injection schedule for first acid fracturing stage of Well A.....	35
Table 3.3: Reservoir and fracture properties - Well B.....	41
Table 3.4: Formation properties - Well C.....	46

CHAPTER I

INTRODUCTION AND LITERATURE REVIEW

Introduction

Acid fracturing is a well stimulation method to improve the productivity of wells in carbonate formations. Injecting the stimulation fluid at above the closure pressure results in the failure of the rock and initiation of a fracture that increases the formation contact with the wellbore. The acid, on the other hand, reacts with the rock to dissolve the interior face of the fracture, resulting in etched faces that help prevent the fracture from closing completely when the pressure goes below the closure pressure. The formation of a long etched fracture improves the productivity of the well significantly.

There are several differences between propped hydraulic fracturing and acid fracturing. Acid fracturing is relatively easy to pump, and there is no worry about screen out. It is also more economical compared with propped fracture. Acid fracturing is limited to carbonate formations, and the fracture is maintained by etching the interior faces of the fracture (Figure 1.1). In addition, it is hard to obtain long fractures because of the high leakoff and spending of treating fluids as they react with the rock. On the other hand, proppant in hydraulic fracturing helps in maintaining the fracture conductivity by preventing the fracture from closing. Furthermore, hydraulic fracturing can be used to stimulate sandstone and shale reservoirs.



Figure 1.1: Role of etching in maintaining fracture width (Kalfayan, 2007)

Acid fracturing is preferable in shallow and low-temperature carbonate reservoirs. Low temperature reduces the reaction rate and allows the treatment fluid to go deep into the formation. Low in-situ stresses are required to maintain modest conductivity of the fracture. However, acid fracturing is better in deep high-temperature reservoirs when the well is damaged due to the contamination of drilling fluids around the wellbore. Moreover, reservoirs with natural fractures such as those rich in dolomite are recommended to be stimulated with acid fracturing since proppant exceeds the width of these natural fractures.

Three stages are usually performed to ensure a successful acid fracturing job: preflush, pad-acid injection and overflush. In the preflush stage, the treatment fluid is injected above the closure pressure to initiate the fracture. The pad-acid injection stage is responsible for propagating the fracture and etching the fracture faces by injecting the pad and acid in stages. Finally, the overflush fluid is injected to push the acid deeper into the formation to react with the rock and eventually increase the porosity and permeability near the fracture.

During all stages, surface gauges record the pressure at the surface, which can be used to estimate the bottomhole pressure with high accuracy. Sometimes downhole gauges are installed to monitor the pressure, but this is usually difficult because of the harsh environment downhole in acid fracturing. These pressure data can provide information of downhole treating condition. Work has been done previously to qualitatively represent some pressure behavior regarding fracture propagation.

In practice, the height of the fracture at the wellbore can be determined using temperature and radioactive logs. Seismic data can also be used as an indication of the fracture geometry. Production data help assess the efficiency of a fracturing job where transient pressure testing can be applied. However, all these techniques are aimed at evaluating the success of the fracturing job and do not predict the ongoing progress of the fracturing job. Furthermore, some of these methods do not represent the actual geometry of the fracture but rather an “equivalent fracture” derived from logs and seismic data.

In this thesis, a systematic methodology is presented to predict the performance of acid fracturing jobs in horizontal wells. The method analyzes the treatment bottomhole pressure above and below the closure pressure. The quantitative analysis is presented by predicting the fracture evolution during the treatment, which is an important measure of the success of acid fracturing job. This methodology is applied to three case studies and the results are compared to the ones from production data analysis.

Field application of the proposed technique shows the effectiveness and importance of the approach in monitoring acid fracturing injection pressure. Immediate interpretation of the data to predict the performance is vitally helpful. In addition,

simplicity of the parameters needed to evaluate the fracture area makes the procedure easier to apply. This means that rather than geomechanical properties of the formation, only some parameters that can be obtained by lab measurements are needed. Furthermore, the calculations are performed under in-situ conditions which result in more accurate results than with data provided from lab experiments.

Literature review

Monitoring injection pressure data

There are three types of fracture propagation models: Perkins-Kern-Nordgren (PKN), Khristianovic-Geertsma-de Klerk (KGD) and radial fracture propagation models. Nordgren (1972) described the conditions that result in the formation of each type of fracture. PKN fracture propagation can be applied if the length of the fracture is much longer than the height and the fracture height is limited. However, if the fracture height is larger than the length, KGD fracture propagation can be assumed. Perkins et al. (1961) suggested that if the injection is over a limited interval, radial fracture propagation can be assumed.

Daneshy (1973) tried to relate the fracture pressure to its parameters. He suggested a method for predicting fracture geometry, the KGD fracture propagation model, which makes an assumption of power-law model instead of Newtonian. He presented some charts showing changes of fracture length and width over time for different fracture propagation models.

Nolte et al. (1981) were the first to discuss pressure response in hydraulic fracturing. Their work combined material balance, fluid flow and fracture compliance relations to derive the relationship between wellbore fracturing pressure and pumping time (Ayoub, 1992). Different slopes in log-log plots of P_{net} ($P_{inj} - P_{closure}$) versus time were interpreted assuming the PKN fracture propagation model. The explanations for different slopes will be discussed in later sections of this work. The results presented in Nolte et al. (1981) are really helpful for understanding fracture propagation during a fracturing job.

Nolte (1988) explained the reason behind the PKN fracture propagation model. He realized a consistent increasing pressure trend for 60 treatments performed in 20 different formations at depths of more than 4,000 ft. In addition, he believed that under the conditions of normal gradients and for formations deeper than 1,750 ft., no slippage between formations is expected, which is different than the assumptions of the KGD fracture propagation model.

Marcos (1997) was interested in analyzing pressure in hydraulic fracturing. He tried to enhance Nolte's methodology by simplifying Carter's equation to make the calculation of fracture volume simpler and more explicit.

Ayoub et al. (1992) introduced the analysis of pressure derivative behavior during fracturing treatments. The work addressed the importance of determining accurately the time origin and closure pressure since they affect the slopes in the pressure analysis. A method for determining the accurate closure pressure using pressure derivative data was introduced. Besides the advantage of helping assess the success of the treatment, the sensitivity of pressure derivative data indicates and magnifies events earlier than does

pressure data. In addition, pressure derivative data are not affected by the incorrect values of closure pressure. Different interpretations of pressure derivative are going to be discussed further in this thesis.

Conway et al. (1985) classified wells into five well types based on treatment pressure behavior. After four years of studying pressure behavior, they believed that pressure behavior can be predicted if the well classification is known. The effect of natural fractures on pressure behavior was discussed. Furthermore, the importance of determining accurately the closure pressure was addressed and a new method was introduced to determine this value.

Fall-off tests are used to determine some of the formation geomechanical properties. The study of various interpretations of pressure responses can be beneficial for this thesis's scope. Liu and Economides (2015) summarized the interpretation of different pressure behaviors in Fall-off tests. These interpretations can be used when the treatment pressure declines to fall below the closure pressure.

Ueda (2015) tried to analyze the pressure injection data in acid fracturing. He used the transient dual porosity solution to estimate fracture area evolution during treatment. He used the bilinear analytical model because of the belief that this is the dominant flow regime during injection. The slab matrix linear model introduced by Bello (2009) was used and modified to adapt to the injection conditions. His results were compared to production data to test the reliability of the proposed method.

Production data analysis

Many papers and publications discuss the ability to determine fracture parameters in horizontal wells. Several techniques and plots can be used to interpret different pressure behaviors in production data to estimate the fracture parameters. These well-known techniques are going to be applied to the production data to confirm the results obtained from the proposed monitoring injection pressure analysis.

El-Banbi (1998) studied well performance in tight gas wells. He reported the well-known characterization of linear flow regime by half-slope in the log-log plot of production pressure or reciprocal of production rate versus time. The work of Nott and Hara (1991) concerning the ability of calculating the fracture half-length using the cumulative oil produced versus time plot was discussed in El-Banbi's dissertation. Different flow regimes were analyzed, and he stated that the appearance of linear or bilinear flow depends on the conductivity of the fracture.

Bello (2009) concentrated on transient analysis of linear behavior in Shale Gas. He discussed five flow regimes and the parameters that can be calculated from their analysis. Slab matrix geometry has been used in the transient solution since it was the most common matrix geometry used in the literature. Beside analyzing production data, Bello's work – which is an extension to El-Banbi's – has potential to be modified to adapt to injection conditions; as seen in Ueda (2015).

Cheng and Raghavan (2013) identified the characteristics of horizontal wells with transverse fractures using the model presented by Raghavan et al. (1997). Three flow regimes were highlighted, and specific parameters were calculated for each. The flow

regimes discussed in their work are bilinear, linear and radial. Fracture half-length is suggested to be calculated using the slope at the linear flow regime period.

Research objectives

After looking thoroughly into the literature for previous work on monitoring injection pressure data for acid fracturing jobs, it is necessary to form a systematic way of analyzing pressure data to assess the efficiency of the job. The analysis can be quantitative, which is preferable to qualitative in case quantitative is impossible to obtain. Topics such as production data analysis, transient pressure analysis, real-time monitoring of matrix acidizing, injection falloff calibration, and pressure analysis for hydraulic fracturing will be investigated. In addition, the only work that has been conducted on this topic (Ueda, 2015) will be investigated and expanded.

The main objectives of this research are as follows:

- 1- Provide a methodology for analyzing monitored injection pressure data to examine the success of acid fracturing jobs. This methodology will indicate whether the fracture is propagating or instead the treatment is just matrix acidizing. During fracturing, the methodology estimates the propagation of the fracture and determines some of the fracture parameters.
- 2- Test the methodology on different field cases to study the reliability and applicability of the proposed method.
- 3- Analyze production data for the same field cases and compare the results with the ones from the proposed method.

CHAPTER II

DEVELOPMENT OF THE METHODOLOGY

Monitoring injection pressure

The goals of this work are to understand the monitored pressure responses and to try to identify some of the fracture parameters, especially fracture area. Some topics that were integral to this study; besides the work done by Ueda in monitoring acid fracturing pressure data; are transient pressure analysis, real-time monitoring of matrix acidizing, injection falloff calibration and pressure analysis for hydraulic fracturing. The results and applicability from the investigation for each topic will be presented. After that, the proposed methodology will be illustrated.

Hydraulic fracturing pressure analysis

Analyzing the hydraulic fracturing pressure is the most important topic to investigate because of the obvious similarity to acid fracturing. There are some differences, such as the reaction of injected fluids in acid fracturing with the formation rock and the usage of proppant in hydraulic fracturing. However, the nature of both jobs where the fluids are injected into the formation in addition to the similarity of injected fluid properties are good reasons to assume similarity between the two jobs. Furthermore, low reaction rate with the rock compared to high injection rate supports this assumption.

Understanding different types of fracture geometry and the pressure response of each fracture is essential. There are three fracture propagation models in hydraulic

fracturing that describe the final geometry and the way that fractures propagate: radial, KGD and PKN models.

The PKN model suggests that the pressure is linearly proportional to time to the n th power, where n is a positive number between 0.13 and 0.25. This means that plotting the difference between injection pressure and closure pressure versus time in a log-log plot will result in a positive slope that is within the range of 0.13 to 0.25. The upper bound is for the assumption of small fluid loss, while the lower one is for large fluid loss rate. The general shape of a PKN fracture is elliptical (Figure 2.1). Nolte (1988) found that the PKN model is preferable in hydraulic fracturing pressure analysis because it is consistent with his review of over 60 treatments from 20 different formations. The assumptions for the PKN propagation model are:

- The fracture height is limited and the length of the fracture is much greater than the height.
- No slippage at the boundary between the targeted formation and confining ones.
- The fracture width is not sensitive to rock properties. However, width is inversely proportional to the Young's modulus to the one fourth power.

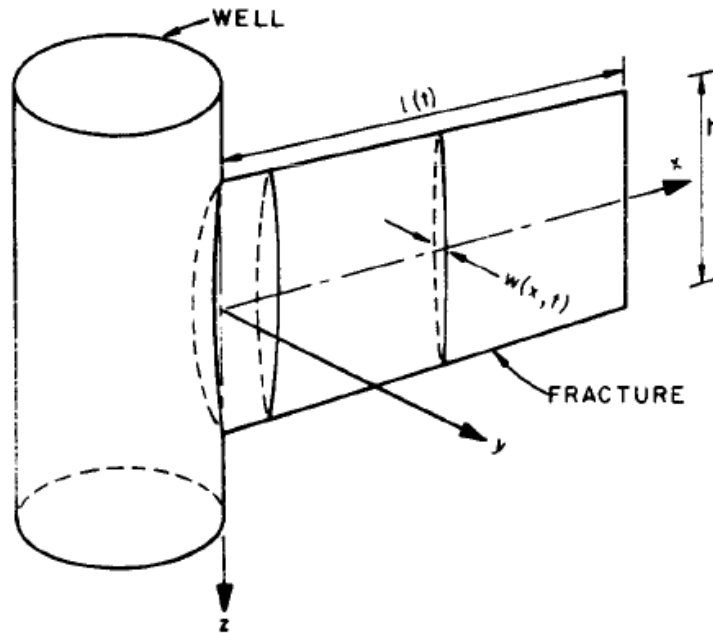


Figure 2.1: PKN fracture geometry (Geertsma et al., 1969)

On the other hand, the KGD model states that the pressure decreases when the fracture propagates. That means that plotting P_{net} versus time in a log-log plot will result in a negative slope between -0.167 and -0.3. The shape of a KGD fracture is assumed to be rectangular with constant width vertically (Figure 2.2). Generally, when the fracture length is relatively small compared to the fracture height and the injection is over the whole height, the fracture is expected to follow this model. KGD propagating model assumptions are:

- The width is constant at the wellbore, which means that the formation slips at the boundary of confining formations.
- The rectangular propagation is assumed when the injection is performed over a long perforated interval to form a line source.

- The height of the fracture during propagation is constant.

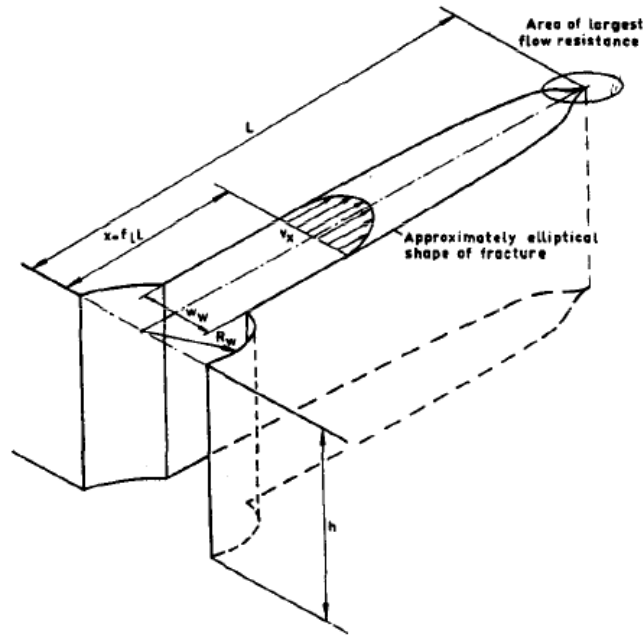


Figure 2.2: KGD fracture geometry (Greetsma et al., 1969)

Finally, the third fracture propagation model is the radial model. In this model, the pressure behaves similarly to that of the KGD model, where the pressure decreases when the fracture propagates. The slope of that decrease when P_{net} is plotted versus time in log-log axes is similar to the KGD model as well. This type of propagation is expected when the treating fluid is injected through a small perforation along the wellbore. Figure 2.3 illustrates the initiation and propagation of each model.

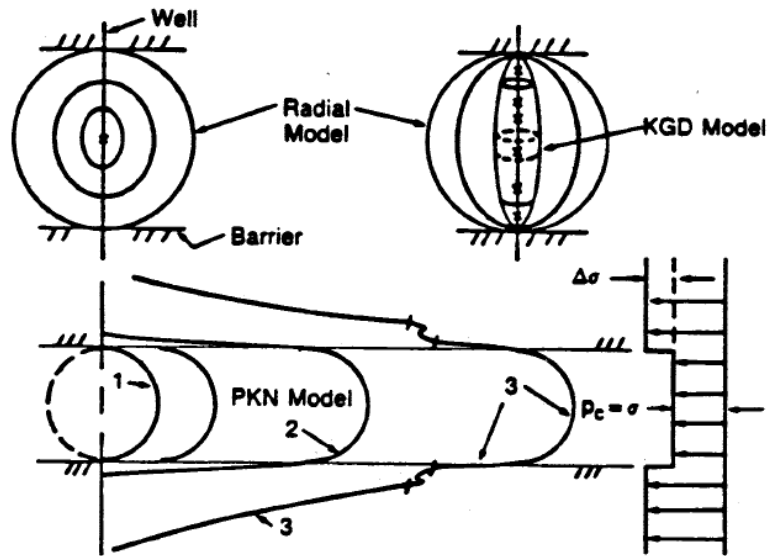
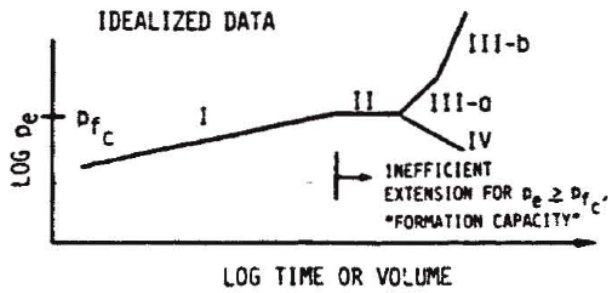


Figure 2.3: Initiation and propagation of different models (Nolte, 1991)

Nolte has conducted extensive work on analyzing fracture pressure data for treatment diagnosis. He mainly used log-log plots of the net pressure ($P_{\text{injection}} - P_{\text{closure}}$) versus time to investigate and interpret different slopes (Figure 2.4). In addition, he tried to relate the fracture pressure to fracture parameters such as the width. He used the PKN propagation model because it is consistent with many treatments that he has analyzed. He classified the behavior of treatment pressure into four modes:

- Small Positive Slope (Mode I): small positive slope that falls between the bounds mentioned previously indicates a propagation that follows the PKN model, with constant compliance and unrestricted extension.

- Constant Pressure (Mode II): This is the most difficult behavior to identify. However, it is also the most critical one since it is usually followed by a sharp increase or decrease. If it is followed by pressure decreasing, an increase in height is the most probable reason for a period of constant pressure. On the other hand, if it is followed by pressure increase, it is probable that the reason is either height increase or fluid loss.
- Unit and Double Slope (Mode III): the unit slope indicates that the pressure is proportional to time, and it is interpreted as a flow restriction in the fracture. The double slope results from a restriction in one wing of the fracture.
- Negative Slope (Mode IV): caused by rapid unstable height growth. However, this is the case if the negative slope appears late in the treatment. Other explanations are given below for situations where the negative slope is noticed at the beginning of the treatment.



APPROXIMATE LOG-LOG SLOPE		INTERPRETATION
1/8-1/4	I	RESTRICTED HEIGHT AND UNRESTRICTED EXTENSION
0	II	a) STABLE HEIGHT GROWTH (ie Moderate) b) FISSURE OPENING
1-1 (UNIT)	III-a	RESTRICTED EXTENSION-two active wings
2-1 (DOUBLE)	III-b	RESTRICTED EXTENSION-one active wing
NEGATIVE	IV	UNSTABLE HEIGHT GROWTH (ie Run-away)

Figure 2.4: Interpretations of different slopes of P_{net} plots (Nolte, 1988)

Ayoub et al. (1992) examined the applicability of using pressure derivative in the log-log plot to interpret different events during treatment. The proposed method suggests that plotting pressure derivative in the log-log plot will result in the same small positive or negative slope from plotting pressure data. However, the value of closure pressure used in pressure data calculations should be correct to give the same slope. Since pressure derivative data are independent of closure pressure, pressure derivative data will help calculate the correct closure pressure by varying the closure pressure value until equal slopes from both plots are obtained. Ayoub et al. addressed the importance of using the correct closure pressure since lower values for closure pressure will result in a flat net pressure plot.

Ayoub et al. (1992) concluded that using pressure derivative has the advantage of magnifying and discovering events earlier in time. For example, in the transition between very early radial propagation and PKN propagation, the pressure derivative plot dips down to almost zero and comes back to the same small positive slope as net pressure plot. Furthermore, pressure derivative shows the exact moment of the end of PKN propagation, while net pressure shows that later in time.

The work done in that paper introduced the response of an important event in hydraulic fracturing: Massive height growth. This means that the fracture breaks a confining barrier to an adjacent formation. A net pressure decreasing behavior is predicted with small pressure derivative values.

As a result of studying pressure behavior in hydraulic fracturing for four years, Conway et al. (1985) presented a well classification method derived from the behavior of treatment pressure. They suggested five well classifications, but two of them are concerned with proppant concentration. The three types that are of interest in my research are:

- Khristianovich: the wells under this classification have a constant pressure behavior plus or minus a slope of 0.05. This type of well is believed to have the fracture perfectly contained within the barriers (Figure 2.5).
- Perkins and Kern: these wells have increasing pressure, with a slope within the bounds of the PKN model. The general shape of such fractures is shown in Figure 2.6. Two potential responses are illustrated in Figure 2.6, and the bottom one is the most common.

- Penny Shaped: This type of fracture is characterized by a continuous decline in pressure followed by a sudden sharp increase. The typical response for such a well and the general shape are illustrated in Figure 2.7.

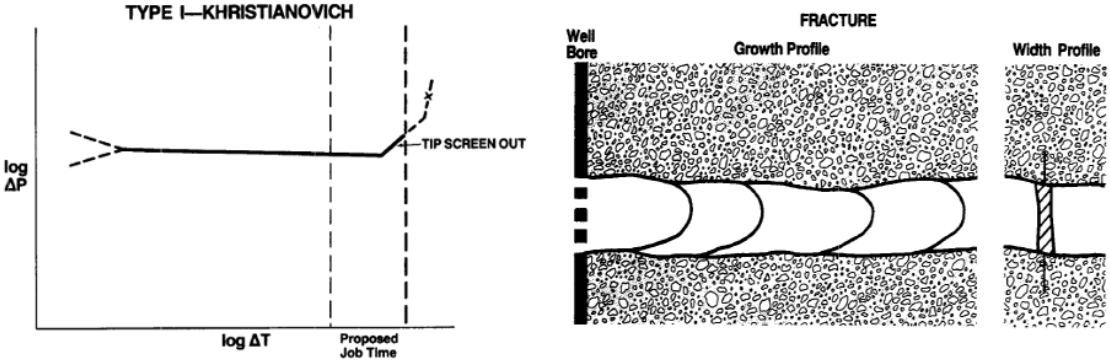


Figure 2.5: Khristianovich fracture (Conway et al., 1985)

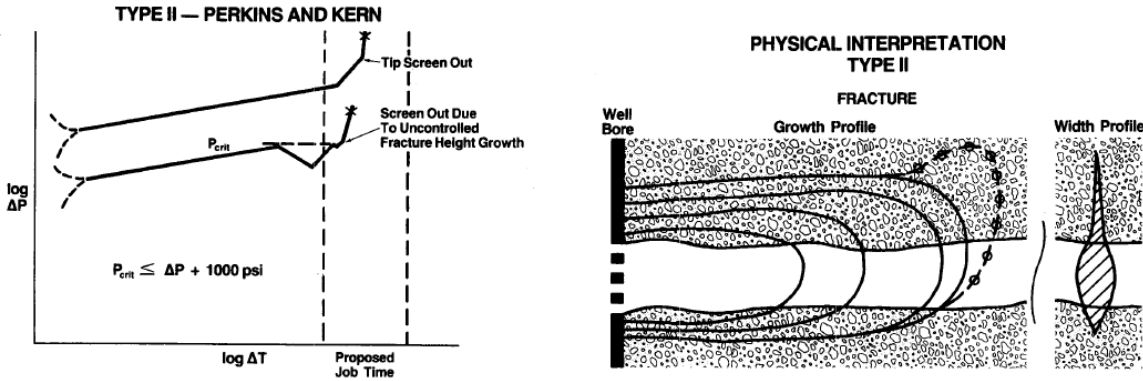


Figure 2.6: Perkins and Kern fracture (Conway et al., 1985)

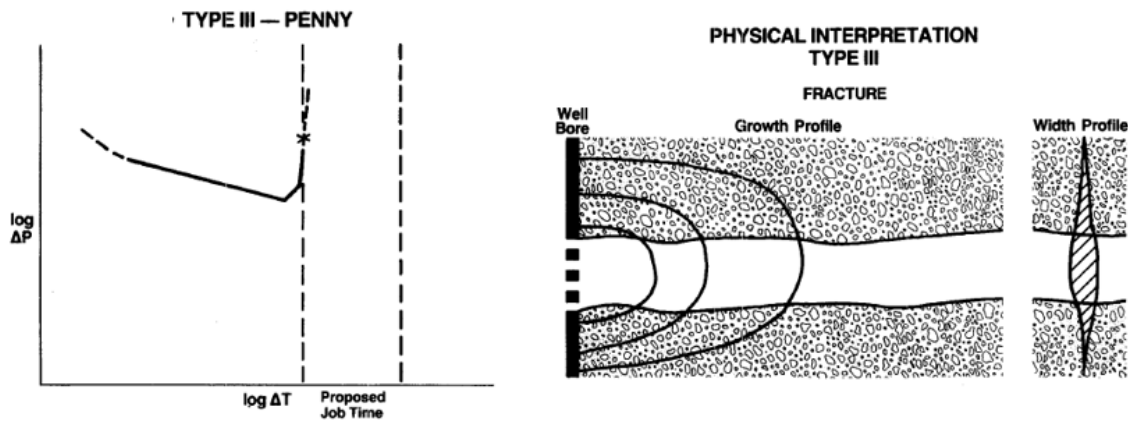


Figure 2.7: Penny fracture (Conway et al., 1985)

After summarizing the work done in hydraulic fracturing pressure analysis, I plan to use the previously published findings to analyze the pressure in acid fracturing treatment. I believe that there is a huge similarity between the two treatments regarding the type of operation performed and the properties of the fluids. Further investigation in the acid fracturing literature will be conducted to study the accuracy of applying hydraulic fracturing findings to acid fracturing. The work done by Nolte (1981) and Ayoub et al. (1992) will be applied to analyzing acid fracturing pressure data in order to analyze the propagation of the fracture during the treatment. In addition, well classification performed by Conway et al. (1985) can be considered in order to evaluate the general shape of the fracture.

Unfortunately, calculating fracture parameters such as fracture area cannot be accomplished using the exact same methods as those used on hydraulic fracturing in previous work. PKN and KGD models provide equations that show the relationship between pressure and fracture parameters such as width, height and length. However,

these equations have some geomechanical parameters that are hard to identify, and using these parameters is beyond the scope of my work.

Acid fracturing

Due to the difficulty of monitoring bottomhole pressure using downhole gauges in acid fracturing, surface pressure is used to estimate it via the equation proposed by Ueda et al. (2016). By adding the effects of friction, the perforation pressure drop and the hydrostatic column pressure to the surface pressure, downhole pressure can be estimated using the following equation:

$$P_{sandface} = P_{surf} + \Delta p_{PE} - \Delta p_f - \Delta p_{near-well} \dots\dots\dots(1)$$

where P_{surf} is the surface recorded pressure, ΔP_{PE} is the hydrostatic pressure column drop, ΔP_f is the frictional pressure drop in tubing, and $\Delta P_{near-well}$ is the perforation pressure drop. In fact, friction reducers are added to the viscous treatment fluids; this makes calculation of friction pressure drop difficult. However, history matching of bottomhole pressure can confirm the right values.

The work done by Ueda (2015) was the first to monitor treatment pressure data in acid fracturing. His main idea was to adopt the transient solution proposed by Bello (2009) to estimate the fracture area for areas that show bilinear flow regime (quarter slope). He used the dual porosity solution for the slab matrix model. His assumption of bilinear flow was proven by simulation model, and two simultaneous linear flows were assumed: one in the fracture and the other into the matrix. The derivation of his proposed methodology is presented below.

The dimensionless constant rate solution for bilinear flow (Bello, 2009) is:

$$p_{DL} = \frac{9.123}{\lambda_{Ac}^{0.25}} t_{DAc}^{0.25} \dots\dots\dots(2)$$

where λ_{Ac} is the dimensionless interporosity parameter and t_{DAc} is the dimensionless time.

The definition of the dimensionless variables is:

$$t_{DAc} = \frac{0.000264 k_f t}{(\phi \mu c_t)_{f+m} A_{cs}} \dots\dots\dots(3)$$

$$p_{DL} = \frac{k_f \sqrt{A_{cs}} (p_i - p_{wf})}{141.2qB\mu} \dots\dots\dots(4)$$

where k_f is fracture permeability (md), t is time (hours), ϕ is porosity, μ is viscosity (cp), c_t is total compressibility (psi⁻¹), A_{cm} is the total matrix surface area draining into the fracture system (ft²), p_i is initial reservoir pressure (psi), p_{wf} is bottomhole flowing pressure (psi), B is formation volume factor (RB/STB) and q is flow rate (STB/day).

Substituting Eq. 4 into Eq. 2:

$$\frac{k_f \sqrt{A_{cs}} (p_i - p_{wf})}{141.2qB\mu} = \frac{9.12305}{\lambda_{Ac}^{0.25}} t_{DAc}^{0.25} \dots\dots\dots(5)$$

Rearranging Eq. 5:

$$\frac{p_{wf} - p_i}{q} = \frac{141.2B\mu}{k_f \sqrt{A_{cs}}} \frac{9.12305}{\lambda_{Ac}^{0.25}} t_{DAc}^{0.25} \dots\dots\dots(6)$$

Substituting Eq. 3 into Eq. 6:

$$\frac{p_{wf} - p_i}{q} = \frac{141.2B\mu}{k_f \sqrt{A_{cs}}} \frac{9.12305}{\lambda_{Ac}^{0.25}} \left[\frac{0.000264 k_f}{(\phi \mu c_t)_{f+m} A_{cs}} \right]^{0.25} t^{0.25} \dots\dots\dots(7)$$

Dimensionless interporosity parameter is defined as:

$$\lambda_{Ac} = \frac{12 k_m}{L^2 k_f} A_c \dots\dots\dots(8)$$

where k_m is matrix permeability (md) and L is general fracture spacing (ft). Substituting Eq. 8 into Eq. 7 results in:

$$\frac{p_{wf} - p_i}{q} = \frac{1}{A_{cs}} \frac{141.2B\mu}{\sqrt{k_f}} \frac{9.12305\sqrt{L}}{(12k_m)^{0.25}} \left[\frac{0.000264}{(\phi \mu c_t)_{f+m}} \right]^{0.25} t^{0.25} \dots\dots\dots(9)$$

Since the flow rate varies during the treatment, bilinear superposition time is used:

$$\Delta t_{sup} = \sum_{j=1}^N \frac{q_j - q_{j-1}}{q_N} (t_N - t_{j-1})^{0.25} \dots\dots\dots(10)$$

The slope m is calculated to be:

$$m = \frac{141.2B\mu}{\sqrt{k_f}} \frac{9.12305\sqrt{L}}{(12k_m)^{0.25}} \left[\frac{0.000264}{(\phi \mu c_t)_{f+m}} \right]^{0.25} \dots\dots\dots(11)$$

where μ is viscosity of the reservoir fluid (cp). Substituting the slope and superposition time into Eq. 11:

$$\frac{p_{wf} - p_i}{q} = \frac{1}{A_c} m \Delta t_{sup} \dots\dots\dots(12)$$

where q is the flow rate of injected fluid (Bbl/day). Finally, cross-sectional area to flow is calculated using:

$$A_c(t) = \frac{m \Delta t_{sup}}{\frac{p_{wf} - p_i}{q}} \dots\dots\dots(13)$$

The same equations are applied for both gas and oil wells.

In the acid fracturing literature, the effect of different parameters on the conductivity, acid penetration in the fracture and leak-off velocity has been discussed. Type of acid plays an important role in fracture propagation. Straight acid results in very high fracture conductivity because of the high reaction rate, but the acid does not penetrate deep in the fracture. On the other hand, the use of gelled acid results in lower fracture conductivity but moderate fluid penetration through the fracture. Finally, emulsified acid results in the lowest conductivity but the deepest fluid penetration.

Since the leak-off velocity is not influenced by injection rate, deeper penetration of treatment fluid inside the fracture is obtained when injection rate increases. In addition, more fracture area contribution to the leak-off is expected in dolomite formations because of the low reactivity compared to calcite. Formation permeability and porosity increase the leak-off rate, resulting in high conductivity but shallow fluid penetration.

Hill et al. (1995) addressed the impact of wormholing on the fluid-loss coefficient. They stated that ignoring the effect of wormholing results in underestimating the leak-off velocity and hence overstating the fluid penetration. Wormholing effect is negligible in dolomite formations because of the high pore volume needed to breakthrough. However, they proved that an increase of 100% in the leak-off coefficient can happen, especially for gas wells in calcite formations.

The methods from previous work in estimating bottomhole pressure and monitoring treatment pressure data will be used in my proposed methodology. The proposed changes to Ueda's (2015) methodology will be explained later in this chapter.

The effect of different parameters on acid penetration through the fracture will be considered in evaluating the calculated fracture area.

Real-time monitoring of matrix acidizing

The work regarding this subject was presented by Hill and Zhu (1996). Their method basically analyzes the inverse injectivity versus superposition time plot to calculate the evolution of the skin factor. A radial flow regime is assumed during the treatment and hence a radial superposition time is used. The assumption of a radial flow results in a unit slope behavior in the log-log plot.

It is concluded from their work that radial flow regime during acid treatment is an indication of matrix acidizing. As a result, this work can be applied in my work by testing for unit slope in the inverse injectivity plot to predict periods of matrix acidizing. Although the ultimate goal of acid fracturing is to propagate a long etched fracture, sometimes the pressure can go way below the closure pressure, causing the fracture to close and matrix acidizing to commence.

Pressure-transient injection and falloff data

Pressure-transient injection data seemed to be an interesting topic to investigate because of the huge similarity in pressure condition. The effect of fracture initiation and propagation in pressure-transient analysis may be helpful to the proposed work. However, the nature of slow propagation of fracture in water injection wells does not affect sufficiently the general radial flow regime in injection wells.

An important conclusion from the injection pressure-transient subject is that early injection data are dominated by outer-zone properties, with no apparent effects of the injected fluids (Larsen et al., 1994). This conclusion will be applied in the modification to Ueda's (2015) methodology.

Falloff data, on the other hand, is a subject that could be helpful to the scope of my research because of the possibility of pressure decrease during acid fracturing treatment to pressure values less than the closure pressure. Interpretation of different flow regimes was attempted from the point of view of this subject. Typical interpretations of linear, bilinear and radial flow were discussed considering this subject. However, a new interpretation of a $3/2$ slope was addressed as a poroelastic closing process. This type of interpretation could be useful in this research.

Proposed methodology

There are some assumptions that will be addressed and justified at each step. However, the main assumption that justifies the use of hydraulic fracturing analysis in this work is a negligible effect of acid reaction with the formation rock. This assumption is valid because of the very high injection rate compared to the reaction rate. This assumption is even more reasonable when fluids that slowly react with the formation, such as gelled acids, or non-reacting fluids such as gelled pads, are used in the treatment.

The reaction of treatment fluids with the formation affects the conductivity and fluid penetration, but the variation in leak-off rate is still considered in the methodologies proposed for hydraulic fracturing. In addition, the effect of reaction diminishes as the acid

is retarded by using gelled or emulsified acids and the percentage of calcite decreases. In fact, most of the acid used in the industry is retarded because of dealing with deep reservoirs with very high temperature. With all these facts in mind, neglecting the effect of reaction is reasonable, and special cases where reaction rate should be considered will be highlighted.

First of all, bottomhole pressure is calculated using Eq. 1 if not measured directly. After that, two plots are prepared and analyzed at the same time. The first plot is the log-log plot of P_{net} (pressure above closure) versus time and the second one is the log-log plot of inverse injectivity ($\Delta p/q$ or $\Delta m(p)/q_{\text{sc}}$) versus time. The pressure above closure plot is analyzed when treatment pressure is above the closure pressure to investigate the propagation of the fracture. If not, the inverse injectivity plot is analyzed to identify different flow regimes. However, there are some cases where the inverse injectivity plot is analyzed while treatment pressure is above closure, which will be discussed later.

To construct the first plot, the closure pressure is needed, and it can be determined either in the lab by performing Differential Strain Curve Analysis on core samples or in-situ by performing tests before the main fracturing treatment. Both P_{net} and the derivative should be on the same plot. Whenever a small negative or positive slope that falls within the range of PKN and KGD bounds is realized in the derivative pressure plot, that slope should be the same as for the P_{net} plot. If not, closure pressure should be varied until both plots have the same slope. This step is important because incorrect values of closure pressure will affect the P_{net} plot.

Nolte's (1981) and Ayoub's (1992) method of analyzing pressure above closure pressure is combined and used to understand the evolution and propagation of the fracture in the next step. The derivative plot helps confirm the illustration from P_{net} plot and magnify events. Table 1 summarizes interpretations of different slopes.

Table 2.1: Interpretation of slopes in pressure above closure plot

P_{net}	Derivative	Interpretation
Large negative slope later in the treatment	Negative values	Unstable growth to neighbor zone
Small negative slope	Small negative slope	KGD or radial propagation
Zero slope	Flat (zero slope)	Stable height growth
		Hard to tell but could be fluid loss to opening natural fissures
Changing from negative to positive slope	Values go to zero	Transition from KGD or radial to PKN propagation
Small positive slope	Small positive slope	PKN propagation
Unit slope		No change in the height or length of the fracture but maybe change in the width (Significant flow restriction)
Double slope		Significant restriction in one wing of the fracture

After analyzing the pressure above closure plot, the inverse injectivity plot is analyzed for flow regimes. There are different possible flow regimes to be recognized in this plot. Radial flow can be identified by a unit slope, linear flow by half slope and bilinear flow by quarter slope.

Linear flow is the least probable flow regime to occur for several reasons. First of all, linear flow in the fracture is not possible since it appears usually for a very short time, as mentioned in the literature. In addition, for a matrix linear flow regime to appear, it needs much longer time than the usual duration of stimulation treatments.

Radial flow regime is an indication that treatment fluids are not passing through the fracture anymore. Instead, the injected fluids are flowing through the wellbore radially. The radial flow regime is an indication of matrix acidizing, and the method proposed by Hill and Zhu (1996) can be used to monitor the evolution of skin around the wellbore if desired. However, if the acid fracturing job is successful, there is no need to calculate the skin around the wellbore since the flow through the fracture will dominate and the fracture skin calculations will be needed.

Bilinear flow regime is expected whenever the conductivity of the fracture is low and a simultaneous linear flow in both the fracture and matrix is happening. This type of flow regime is characterized by a quarter slope pressure log-log plots. Ueda (2015) simulated acid injection into a reservoir with three transverse fractures to prove the existence of bilinear flow regime during injection. He used reservoir and fracture properties similar to the case study he discussed. The diagnostic plots showed a quarter slope, indicating that the flow regime during injection is bilinear.

Bilinear flow is the most likely flow regime to appear during injection when fracture area is constant, for several reasons. The work performed by Ueda (2015) supports the existence of bilinear flow regime during injection. In addition, Bello (2009) addressed in his work of analyzing transient pressure in fractured wells that bilinear flow is the

second flow regime after fracture linear flow which appears for a very short time. Finally, no flow regime in the literature was described for injected fluids through fractured wells. As a result, bilinear flow regime will be expected whenever pressure is high enough to flow fluids through the fracture. This is the case whenever the pressure is above closure pressure. Most importantly, the fracture area should be constant for bilinear flow assumption. Pressure above closure plot should indicate no propagation for pressure data above closure pressure. During this flow regime, etching is occurring in the fracture walls since the treatment fluids react with the fracture face.

The methodology presented by Ueda (2015) was investigated and studied to evaluate its applicability to this work. With modifications that is going to be discussed, his work can be applied for bilinear flow regime periods to calculate fracture area. However, some points should be taken into consideration with the values obtained from applying this method. First of all, flow rate plays an important role in flowing the injected fluids through the fracture since higher flow rates result in deeper penetration in the fracture. As a result, the obtained fracture area can represent a portion of the fracture if the flow rate is not high enough. Second, other factors such as permeability, porosity, acid strength, lithology and wormholing should be considered when discerning whether the calculated fracture area represents the real one or only part of it. In general, high permeability, high porosity, use of strong acids, and wormholing reduces the penetration of acid in the fracture, resulting in smaller fracture area. The wormholing negative effect is the most when strong acids are used to stimulate gas wells in calcite formations. Fortunately, most acid fracturing jobs are performed for tight formations using either

gelled or emulsified acids, making the obtained fracture area represent the total fracture area.

Because of the important conclusions obtained from the injection pressure-transient topic mentioned before, there are different sets of equations used for oil and gas wells. The derivation of the equations for gas wells will be addressed; then the final equations for oil wells will be presented.

The dimensionless constant rate solution for bilinear flow (Bello, 2009) is:

$$p_{DL} = \frac{9.123}{\lambda_{AC}^{0.25}} t_{AC}^{0.25} \dots\dots\dots(2)$$

where λ_{AC} is the dimensionless interporosity parameter and t_{DAc} is the dimensionless time.

The definition of the dimensionless variables is:

$$t_{DAc} = \frac{0.000264 k_f t}{(\phi \mu c_t)_{f+m} A_{cs}} \dots\dots\dots(3)$$

$$m_{DL} = \frac{k_f \sqrt{A_c} [m(p_i) - m(p_{wf})]}{1422 q_g T} \dots\dots\dots(14)$$

where k_f is fracture permeability (md), t is time (hours), ϕ is porosity, μ is viscosity (cp), c_t is total compressibility (psi^{-1}), A_{cm} is the total matrix surface area draining into the fracture system (ft^2), p_i is initial reservoir pressure (psi), p_{wf} is bottomhole flowing pressure (psi), q_g is gas rate (Mscf/day) and T is absolute temperature ($^{\circ}\text{R}$). Since the injection pressure is usually above 3,000 psi, the dimensionless pseudo pressure can be replaced with pressure using the following equation:

$$p_{DL} = \frac{k_f \sqrt{A_c} (p_i - p_{wf}) \left(\frac{2p_i}{\mu_i z_i} \right)}{1422q_g T} \dots\dots\dots(15)$$

Substituting Eq. 15 into Eq. 2:

$$\frac{k_f \sqrt{A_c} (p_{wf} - p_i) \left(\frac{2p_i}{\mu_i z_i} \right)}{1422q T} = \frac{9.12305}{\lambda_{Ac}^{0.25}} t_{DAc}^{0.25} \dots\dots\dots(16)$$

Rearranging Eq. 16:

$$\frac{p_{wf} - p_i}{q} = \frac{1422T}{k_f \sqrt{A_{cw}}} \left(\frac{\mu_i z_i}{2p_i} \right) \frac{9.12305}{\lambda_{Ac}^{0.25}} t_{DAc}^{0.25} \dots\dots\dots(17)$$

Substituting dimensionless time into Eq. 17:

$$\frac{p_{wf} - p_i}{q} = \frac{1422T}{k_f \sqrt{A_c}} \left(\frac{\mu_i z_i}{2p_i} \right) \frac{9.12305}{\lambda_{Ac}^{0.25}} \left[\frac{0.000264 k_f}{(\phi \mu c_t)_{f+m} A_c} \right]^{0.25} t^{0.25} \dots\dots\dots(18)$$

Dimensionless interporosity parameter is defined as:

$$\lambda_{Ac} = \frac{12 k_m}{L^2 k_f} A_c \dots\dots\dots(8)$$

Substituting Eq. 8 into Eq. 18 results in:

$$\frac{p_{wf} - p_i}{q} = \frac{1}{A_c} \frac{1422T}{\sqrt{k_f}} \left(\frac{\mu_i z_i}{2p_i} \right) \frac{9.12305 \sqrt{L}}{(12k_m)^{0.25}} \left[\frac{0.000264}{(\phi \mu c_t)_{f+m}} \right]^{0.25} t^{0.25} \dots\dots\dots(19)$$

Since the flow rate varies during the treatment, bilinear superposition time is used:

$$\Delta t_{sup} = \sum_{j=1}^N \frac{q_j - q_{j-1}}{q_N} (t_N - t_{j-1})^{0.25} \dots\dots\dots(10)$$

The slope m is calculated to be:

$$m = \frac{1422T}{\sqrt{k_f}} \left(\frac{\mu_i z_i}{2p_i} \right) \frac{9.12305 \sqrt{L}}{(12k_m)^{0.25}} \left[\frac{0.000264}{(\phi \mu c_t)_{f+m}} \right]^{0.25} \dots\dots\dots(20)$$

where μ is the gas viscosity (cp). Substituting the slope and superposition time into Eq. 19:

$$\frac{p_{wf} - p_i}{q_g} = \frac{1}{A_c} m \Delta t_{sup} \dots\dots\dots(21)$$

where q_g is gas rate (Mscf/day). This parameter can be calculated by multiplying the injected fluid rate by the reciprocal of gas formation volume factor. Finally, cross-sectional area to flow is calculated using:

$$A_c(t) = \frac{m \Delta t_{sup}}{\frac{p_{wf} - p_i}{q}} \dots\dots\dots(13)$$

For oil wells, the slope is calculated using Eq. 11:

$$m = \frac{141.2 B \mu}{\sqrt{k_f}} \frac{9.12305 \sqrt{L}}{(12 k_m)^{0.25}} \left[\frac{0.000264}{(\phi \mu c_t)_{f+m}} \right]^{0.25} \dots\dots\dots(11)$$

where μ is the oil viscosity (cp). In addition, the flow rate used in Eq. 13 is the oil rate (STB/d). The reciprocal of oil formation volume factor is multiplied by the injection rate to obtain the oil rate.

To make the analysis easier, the fracture area calculation can be applied to the whole treatment period and fracture area profile can be plotted. However, areas of interest, where bilinear flow regimes are realized with no fracture propagation, should be considered. The fracture area is plotted as a profile to realize constant fracture area regions and confirm both that the fracture is constant and the bilinear flow regime exists.

To have an idea about the general shape of the fracture, the previously discussed work of Conway et al. (1985) can be applied. In addition, smart conclusions from pressure above closure can be combined with Conway's (1985) method to predict the final fracture shape. Knowledge of the general shape of the fracture is helpful for determining the height and half length of the fracture.

Finally, to summarize this new methodology of monitoring injection pressure in acid fracturing:

- 1- If bottomhole pressure is not monitored by gauges, bottomhole pressure is calculated.
- 2- Pressure above closure is constructed after correcting for closure pressure.
- 3- From pressure above closure plot, propagation and evolution of the fracture is monitored by analyzing different slopes. For periods where pressure is above closure pressure, etching to the internal faces is expected.
- 4- An inverse injectivity plot is constructed and radial and bilinear flow regimes are investigated.
- 5- If radial flow is recognized, matrix acidizing is anticipated.
- 6- If bilinear flow is realized, fracture area is calculated and etching is expected to occur. Different factors that affect the fluid flow in fracture should be considered in order to make conclusions about the obtained fracture area.
- 7- The general shape of the fracture is studied by looking at the general trend of the pressure above closure plot.

Production data

Evaluating the success of a fracturing job can be done by analyzing build-up tests or production data. Bello (2009) used production data to evaluate horizontal well fracture parameters for shale gas reservoirs and his methods will be used in this study.

The flow regime used to obtain the fracture area when matrix permeability is known is the linear flow regime in matrix. That flow regime can be depicted by ½ slope in the plot of normalized pressure ($\Delta m(p)/qg$) versus square root of time. The slope m_4 is calculated and substituted in the following equation:

$$\sqrt{k_m} A_{cm} = \frac{803.2T}{\sqrt{(\phi\mu c_t)_{f+m}}} \frac{1}{\tilde{m}_4} \dots\dots\dots(22)$$

When matrix permeability is known, fracture area can be calculated.

CHAPTER III
RESULTS AND DISCUSSION

In this chapter, the developed methodology is applied to three field cases to illustrate the procedure.

Well A

Well A is a horizontal well located in a tight carbonate formation. A multi-stage acid fracturing job was designed to improve the productivity of the well. Unfortunately, the goal of obtaining multiple fractures was not accomplished. As a result, only one fracture resulted from the six stages performed. The properties of the reservoir and some fracture parameters are tabulated in Table 3.1. The schedule of the treatment is presented in Table 3.2. The treatment was monitored using surface pressure gauges. Knowing the treatment schedule and fluid properties, bottomhole pressure was calculated.

Table 3.1: Reservoir and fracture parameters for Well A

Reservoir and Fracture Properties	
Parameters	Input Values
Initial Reservoir Pressure	9837 psi
Formation Volume Factor	0.003 ft ³ /scf
Total Porosity	0.03
Total Compressibility	5.78E-05 1/psi
Formation Thickness	250 ft.
Reservoir Fluid Viscosity	0.0315 cp
Reservoir Temperature	270 F
Z Factor	1.36
Matrix Permeability	0.0044 md
Fracture Permeability	2000 D
Fracture Width	0.001 ft.

Table 3.2: Injection schedule for first acid fracturing stage of Well A

Injection Schedule			
Stage	Name	Viscosity, cp	Volume (gal)
1	Gelled Acid	39	18492
2	X-linked acid	30	31701
3	Non-X-linked frac fluid	56	52834
4	X-linked acid	30	36984
5	Non-X-linked frac fluid	56	52834
6	Gelled acid	39	18492
7	Water Flush	1	5283

The pressure above closure plot was prepared using the closure pressure of the formation (Figure 3.1). The flow rate was included in the plot to insure a constant flow rate when studying different slopes. To guarantee the accuracy of the plot, pressure derivative was also included in the plot to study the behavior at early times of the treatment by comparing the early slope of both plots. Unfortunately, the pressure derivative plot did not look reliable; the reason could be the sensitivity of the derivative plot to the bad quality of pressure data.

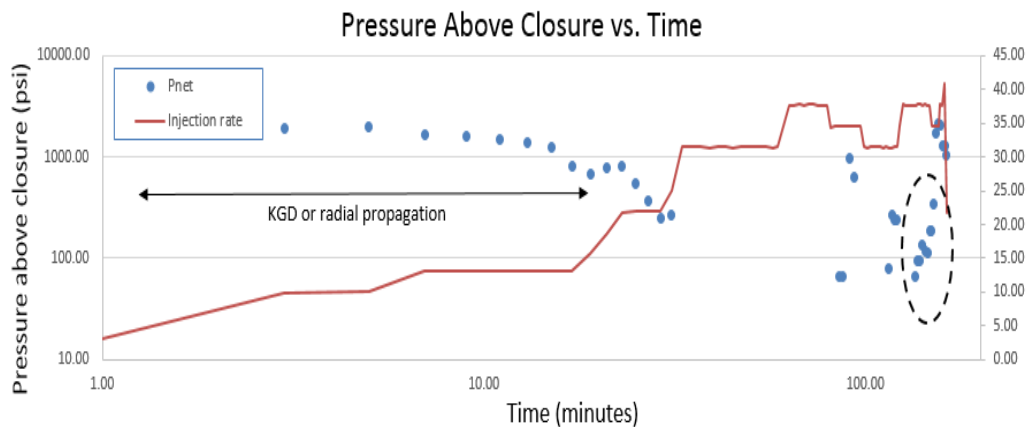


Figure 3.1: Pressure above closure - Well A

As can be seen from the plot, the pressure was above the closure pressure for the first 27 minutes. Wherever the flow rate was constant in that period (the first 17 minutes), a small negative slope was realized, indicating either radial or KGD fracture propagation. For the remaining 10 minutes, the rate kept changing, thus the area could not be interpreted. After that, the bottomhole pressure went below closure pressure for 50 minutes. From the 87th minute until the end of the stage, the pressure kept fluctuating above and below the closure pressure, and finally, in the last twenty minutes, a sharp increase was observed, indicating a propagation restriction.

For the periods where the pressure was below closure pressure or fracture was not propagating, the inverse injectivity plot was studied for further investigation. Quarter or unit slopes were investigated to look for bilinear or radial flow. Three regions were recognized to have quarter slope (Figure 3.2), and the proposed methodology was applied to calculate the fracture area. Two periods have pressure slightly below closure pressure, while the third region exhibits a sharp pressure increase. However, I believe that the pressure did not go below closure pressure but the inaccuracy in closure pressure and bottomhole pressure calculations resulted the disappearing of data in these two periods. The fracture area is calculated to be 74,500 ft² by the end of the stage. Figure 3.3 illustrates the advantages of analyzing the pressure above closure plot, inverse injectivity and fracture evolution plots.

The obtained fracture area is expected to represent the total fracture area for the following reasons. The fluid injected during the third period is non-cross-linked fracturing fluid, which is not reactive to the formation. As a result, other factors that should be

considered to investigate the calculated value are neglected. In addition, the flow rate was high enough to maintain the pressure above closure pressure, which assures the contribution of the total fracture area to the flow.

A sample calculation of fracture area at the third period will be presented. First, the slope m is calculated using Eq. 20:

$$m = \left(\frac{1422 * (270 + 460)}{\sqrt{5}} \right) \left(\frac{0.03155 * 1.356}{2 * 9837} \right) \left(\frac{9.123 * \sqrt{1357}}{\sqrt[4]{12 * 0.0044}} \right) \left[\frac{0.000264}{(0.03 * 0.0315 * 5.78E^{-5}) * 60} \right]^{0.25}$$

$$m = 2,120$$

The bilinear superposition time is calculated at treatment time = 143 minutes, using Eq. 10 to be 3.202 minutes^{0.25}. Substituting these values into Eq. 13:

$$A_c = \frac{(2120 * 3.202)}{\frac{(14766 - 9837)}{(37.8 * 1000 * 0.001 * 60 * 24)}} = 74,900 \text{ ft}^2$$

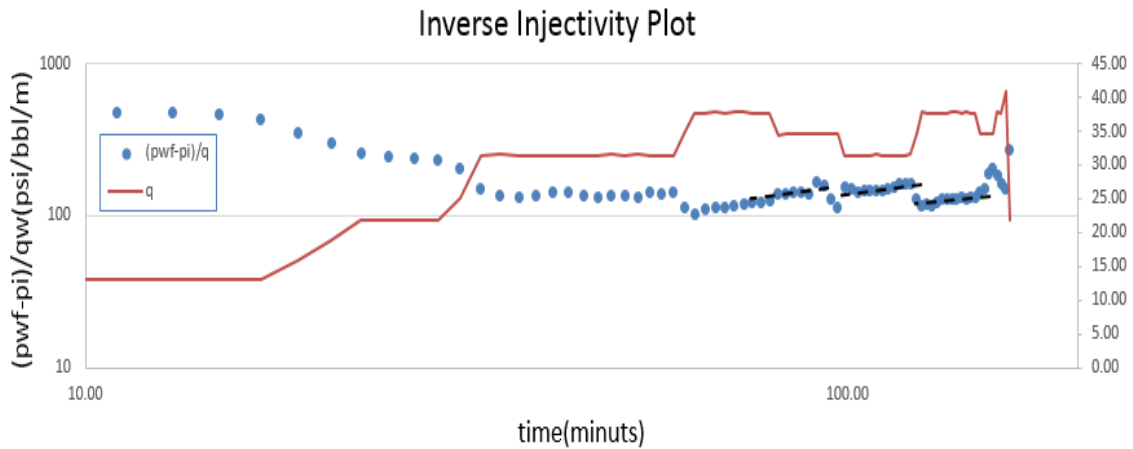


Figure 3.2: Inverse injectivity plot - Well A

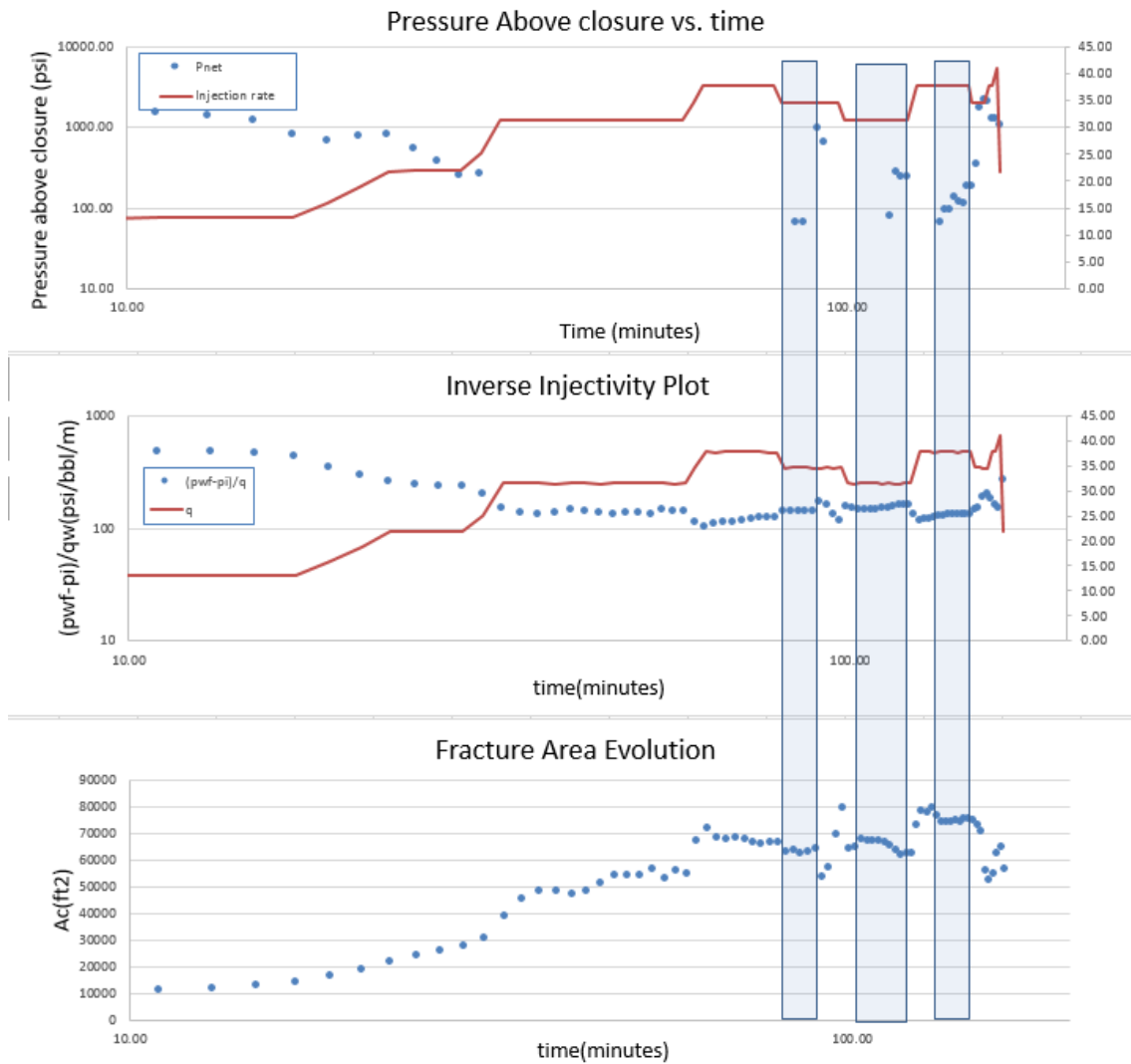


Figure 3.3: Combined plots analysis - Well A

The general shape of the fracture can be predicted to follow either radial or KGD geometry. In addition, the behavior of pressure at the beginning of the treatment is similar to behavior of a penny fracture in Conway's (1985) method. That means that the fracture length is relatively similar to the height. In fact, taking into consideration the high thickness of this formation, it is expected to end up with this final fracture shape.

The production data for 113 days are available and can be used to estimate the fracture area. Since the reservoir is classified as a wet gas reservoir, the combined gas rate should be calculated first using available PVT data. Figure 3.4 shows the production history of this well. The following equation suggested by McCain (1990) can be used to calculate the combined flow rate:

$$Q_{g,wet} = Q_{g,dry} + 133.316(\gamma_o Q_o / M_o)$$

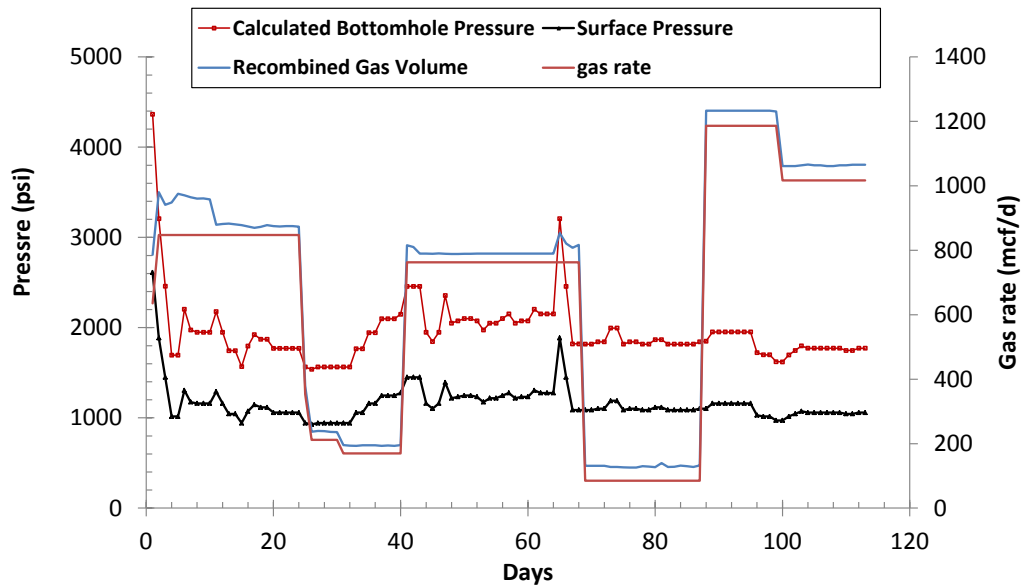


Figure 3.4: Production history for Well A

The real gas pseudo pressure is calculated using bottomhole pressure data. After that, the plot of normalized pseudo pressure versus square root of superposition linear time is constructed (Figure 3.5). A linear trend can be realized and diversion from that trend at the end of production data is observed. After calculating the slope of that straight line, Eq. 22 is used to calculate the fracture area to be 76,200 ft². The obtained fracture area values

obtained from the proposed methodology and from analyzing production data show great similarity, with an error of 2%.

The slope is calculated to be 600,000. This value is substituted into Eq. 22:

$$\sqrt{0.0044} A_{cm} = \frac{803.2 * (270 + 460)}{\sqrt{0.03 * 0.02155 * 5.78E^{-5} * 600000}}$$

$$A_{cm} = 76,200 \text{ ft}^2$$

This result confirms the estimation of fracture area by pressure analysis during fracturing, and the difference between the two estimations is 1.7%.

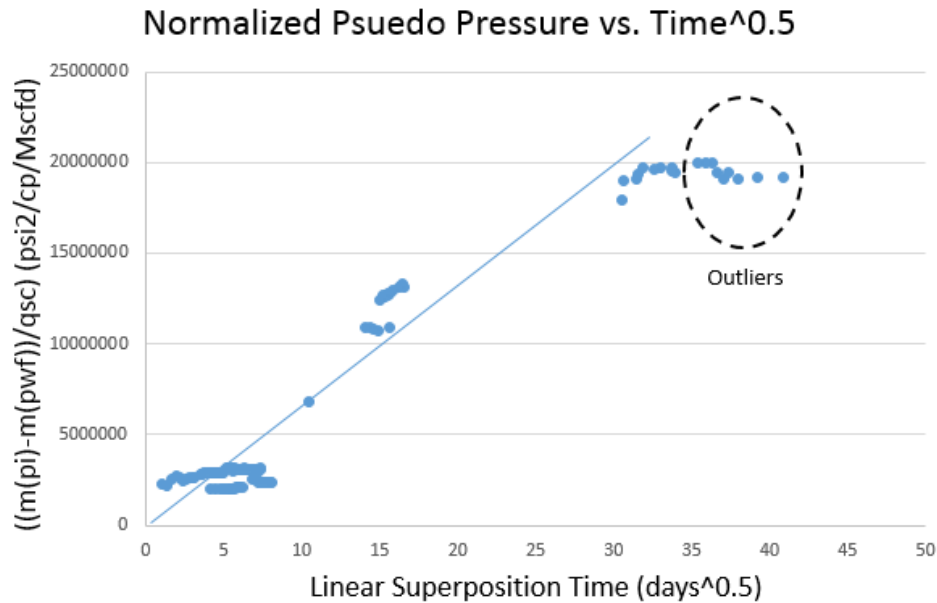


Figure 3.5: Normalized pseudo pressure plot - Well A

Well B

The second well examined is a horizontal well in a carbonate formation. This well was a candidate for a seven-stage acid fracturing. However, only four stages were successful, creating four fractures. The first stage is analyzed because the quality of data

for the other stages is not good. The formation and wellbore parameters are summarized in Table 3.3. Bottomhole pressure data are calculated using surface pressure, and injected fluid properties have been discussed previously.

Table 3.3: Reservoir and fracture properties - Well B

Reservoir and Fracture Properties	
Parameters	Input Values
Initial Reservoir Pressure	10382 psi
Total Porosity	0.02
Total Compressibility	4.6E-05 1/psi
Formation Thickness	250 ft.
Reservoir Fluid Viscosity	0.0392 cp
Reservoir Temperature	280 F
Z Factor	1.48
Matrix Permeability	0.005 md
Fracture Permeability	2000 D
Fracture Width	0.001 ft.

This treatment was performed during most of the period above the closure pressure. In fact, the pressure was higher than the closure pressure throughout the whole treatment; but the different viscosities of different injected fluids disturbed the calculated bottomhole pressure data, resulting in this fluctuation above and below closure pressure. However, this disturbance does not affect the overall quality of calculated pressure.

Figure 3.6 illustrates the pressure above closure trend during the treatment. For the first 26 minutes, the fracture started propagating following the PKN model, then the slope changed to negative, indicating KGD fracture propagation, and finally went back to PKN propagation. After that, the quality of data was poor due to the reason explained

previously, but a sharp increase in the pressure between 110-126 minutes is seen, indicating a propagation restriction.

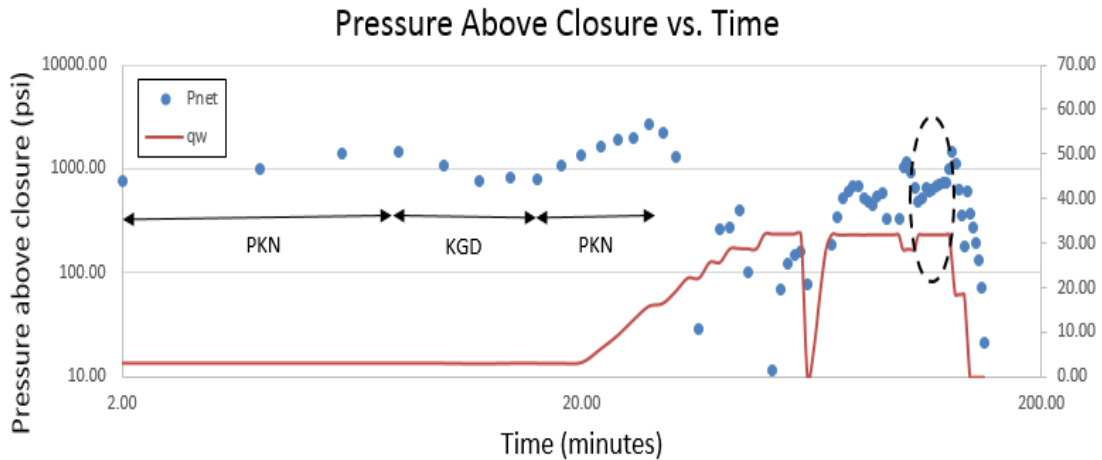


Figure 3.6: Pressure above closure plot - Well B

The inverse injectivity plot (Figure 3.7) shows two bilinear flow regimes. For the first one, the poor data quality does not indicate the situation of the fracture propagation during that period, but the pressure values close to closure pressure make the assumption of constant fracture reasonable. Moreover, the second period is indicated by the pressure above closure plot to have a propagation restriction. As a result, both periods are candidates for applying the new methodology to calculate the fracture area. As can be seen from the combined plot (Figure 3.8), the highest fracture area obtained is 42,500ft². The obtained fracture area is expected to represent the total fracture area for the same reasons explained for Well A. The general shape of the fracture can be assumed to follow the PKN geometry, as the data suggests that it follows the PKN propagation slope during most of

the treatment. In addition, the pressure behavior at the beginning of the treatment indicated a Perkins and Kern final fracture geometry based on Conway's method.

A sample calculation of fracture area at the second period will be presented. First the slope m is calculated using Eq. 20:

$$m = \left(\frac{1422 * (280 + 460)}{\sqrt{5}} \right) \left(\frac{0.03924 * 1.477}{2 * 10382} \right) \left(\frac{9.123 * \sqrt{427}}{\sqrt[4]{12 * 0.005}} \right) \left[\frac{0.000264}{(0.02 * 0.03924 * 4.6E^{-5}) * 60} \right]^{0.25}$$

$$m = 1,665$$

The bilinear superposition time is calculated at treatment time = 118 minutes, using Eq. 10 to be 2.99 minutes^{0.25}. Substituting these values into Eq. 13:

$$A_c = \frac{1665 * 2.99}{\frac{(15755 - 10382)}{(31.8 * 990 * 0.001 * 60 * 24)}} = 42,500 \text{ ft}^2$$

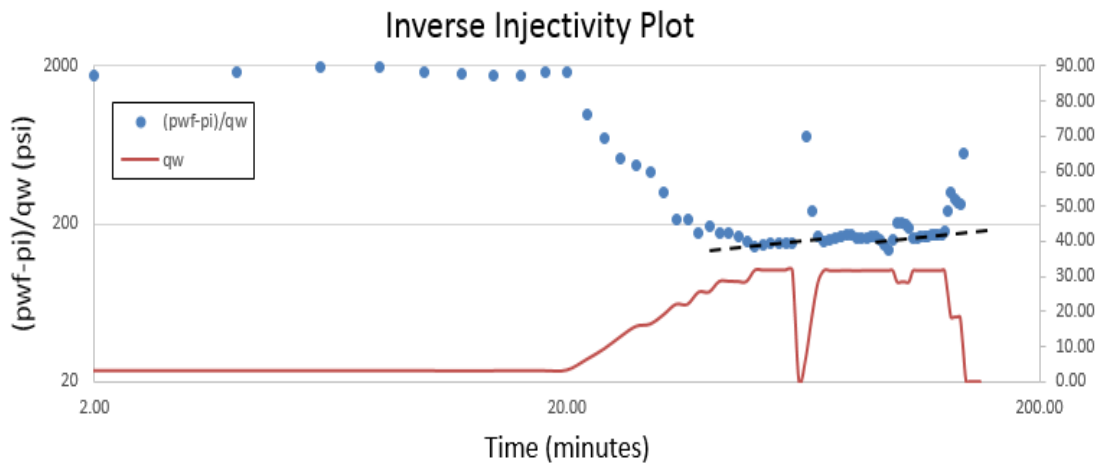


Figure 3.7: Inverse injectivity plot - Well B

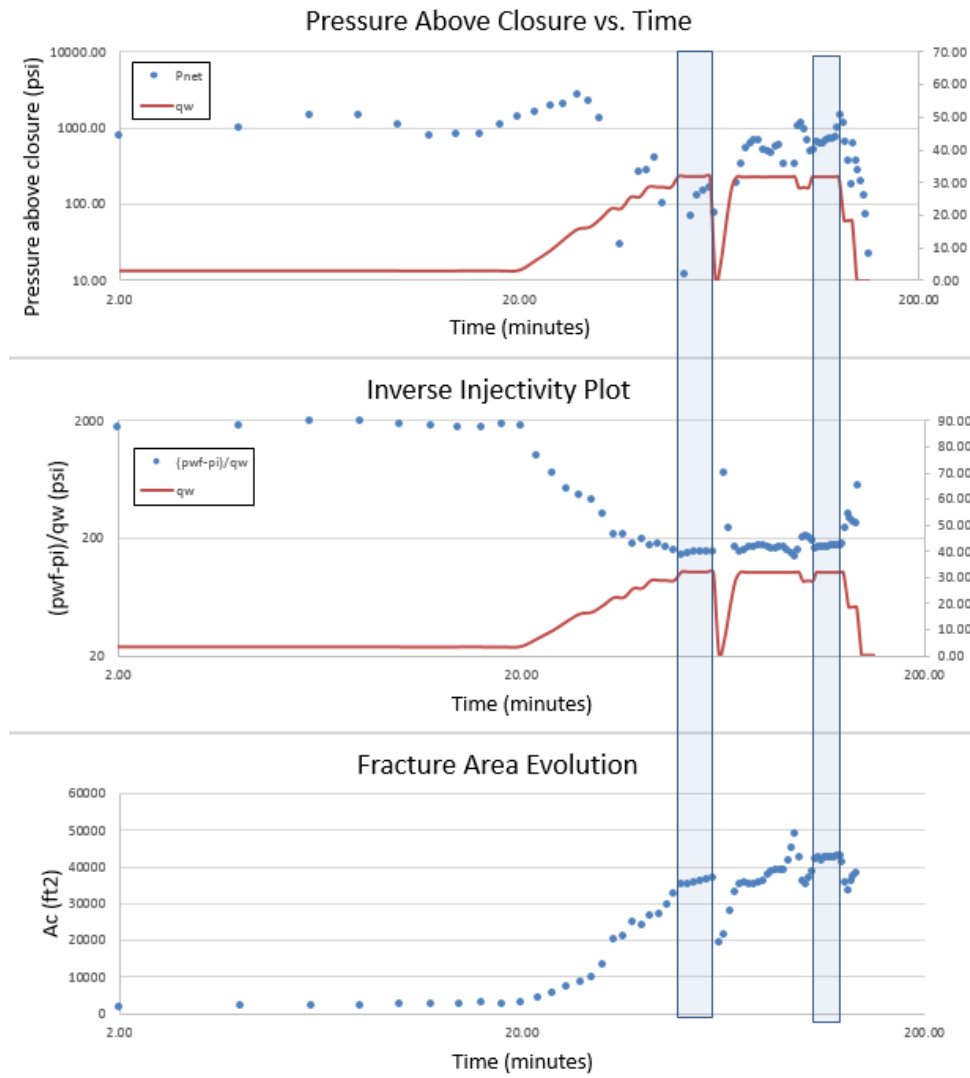


Figure 3.8: Combined plot - Well B

Unfortunately, the production data regarding this well showed very low gas production and high water cut. Furthermore, the production history showed that the well was shut off most of the time. Moreover, even if the production data was provided, it would be necessary to calculate the fracture area of the other successful stages to sum

them and compare them to the one obtained from production data. As a result, confirming the results for this well was not possible.

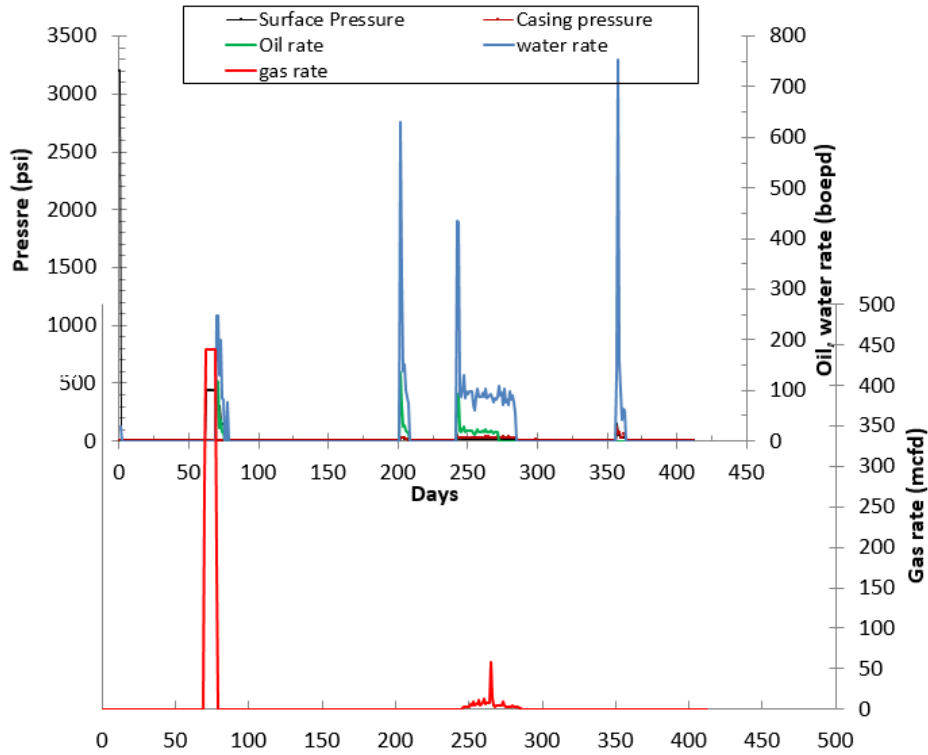


Figure 3.9: Production history for Well B

Well C

Well C is a horizontal well in carbonate formation that was scheduled for matrix acidizing. The reservoir properties are tabulated in Table 3.4. The stimulation schedule consists of the step-rate injection test, the acid injection stage, and finally the overflush stage. During the pre-stimulation step-rate test, the fracture extension pressure and closure pressure was calculated to be 6241 and 5745 psi, respectively. 28% acid was used in the

main acid injection stage. Downhole gauges were used to measure downhole pressure, and the values were corrected for the effect of friction and perforation to calculate the reservoir-face pressures.

Table 3.4: Formation properties - Well C

Reservoir and Fracture Properties	
Parameters	Input Values
Initial Reservoir Pressure	4159 psi
Formation Volume Factor	1.3 Bbl/STB
Total Porosity	0.36
Total Compressibility	9.14E-05 1/psi
Formation Thickness	97 ft.
Reservoir Fluid Viscosity	0.28 cp
Reservoir Temperature	240 F
Matrix Permeability	0.5 md

Figure 3.10 represents the downhole flowing pressure analysis. The acid injection started at the surface at $t = 60$ minutes. However, it took the treatment fluid 8 minutes to reach the reservoir face. That means that fresh water was injected into the formation during this period. The reservoir-face pressure went above the fracture extension pressure, causing the initiation and propagation of a fracture.

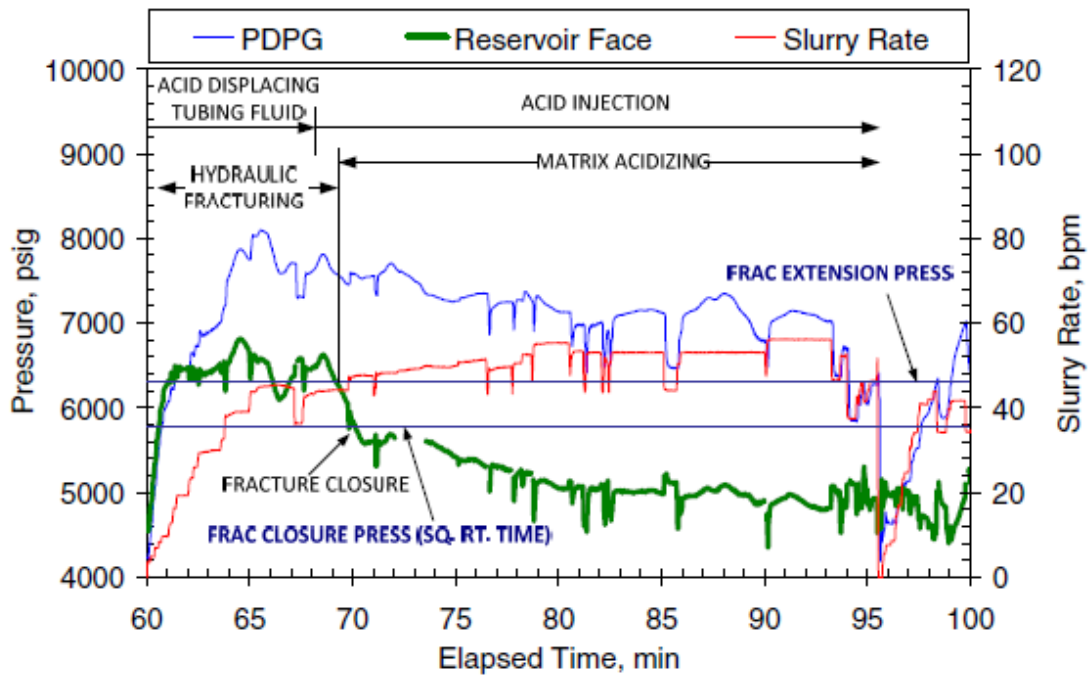


Figure 3.10: Downhole flowing pressure analysis - Well C

The pressure above closure and inverse injectivity plots are prepared (Figure 3.11). From the first plot, a PKN fracture propagation is realized for the first 8 minutes. After that, a sharp pressure drop is observed, indicating treatment fluid entry into the formation. Studying the inverse injectivity plot, an increasing rate between 68-80 minutes makes it hard to determine the flow regime. After that and until the end of the treatment, the declining pressure with unit slope is an indication of matrix acidizing.

As can be seen from Figure 3.10, there is a short period of approximately one minute where the pressure went below the fracture extension pressure but was still above the closure pressure. Furthermore, Figure 3.11 indicates that the fracture area at that period is constant because of the sharp increase in the pressure above closure plot and the quarter slope in the inverse injectivity plot. As a result, the fracture area is calculated during this

period to be 100,000 ft². The final fracture geometry can be predicted to be Perkins and Kern fracture.

A sample calculation of fracture area is presented. First the slope m is calculated using Eq. 11:

$$m = \left(\frac{141.2 * 1.3 * 0.2802}{\sqrt{5}} \right) \left(\frac{9.123 * \sqrt{970}}{\sqrt[4]{12 * 0.5}} \right) \left[\frac{0.000264}{(0.36 * 0.2802 * 9.14E^{-5}) * 60} \right]^{0.25}$$

$$m = 3,470$$

The bilinear superposition time is calculated at treatment time = 7 minutes, using Eq. 10 to be 1.45 minutes^{0.25}. Substituting these values into Eq. 13:

$$A_c = \frac{3470 * 1.45}{\frac{(6659 - 4159)}{(44.8 * 0.77 * 60 * 24)}} = 100,100 \text{ ft}^2$$

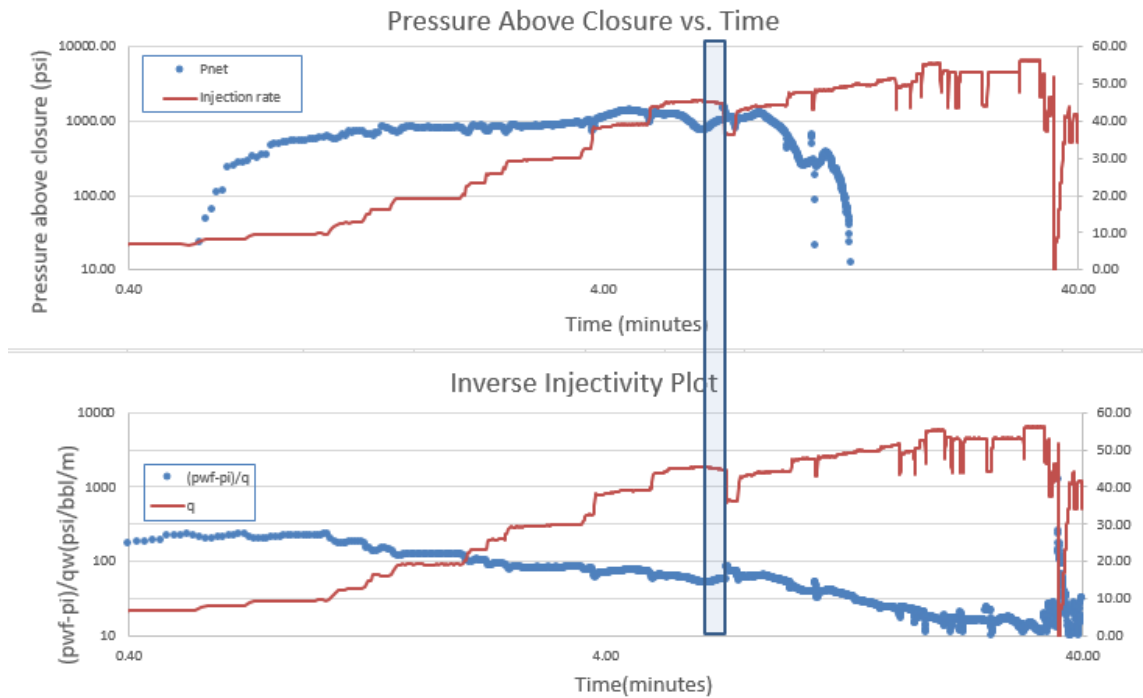


Figure 3.11: Combined plots - Well C

To study the reliability of the obtained fracture area, the work presented by Daneshy (1973) of predicting fracture length for different fracture propagation models was used. After propagating for 7 minutes for a PKN propagation model with reservoir parameters and injection conditions similar to the studied case, the fracture half-length is predicted using Daneshy's work to be 170 ft. Assuming a rectangular shape, the calculated fracture half-length is 250 ft. Because of having the injection rate double the value used to generate the plots in Daneshy's work, it is expected to have a longer fracture half-length. As a result, the predicted fracture area is reasonable.

Discussion

The results obtained from applying the new methodology to the three field cases were promising. Applying hydraulic fracturing principles to acid fracturing turned out to be generally useful. Different slopes realized in hydraulic fracturing were recognized in the cases that were analyzed. Small variations were predicted in the slope values investigated in pressure above closure plots. Two reasons are possibly behind this variation: the inaccuracy in bottomhole pressure calculations and the inaccurate closure pressure estimate. However, the general trends can be identified easily in both case studies.

Applying pressure derivative analysis to the pressure above closure was not successful in the two gas wells discussed because of the high sensitivity of pressure derivative to pressure values. Apparently the calculated bottomhole pressure from surface values was not accurate, and applying derivative to these values resulted in unreasonable

derivative results. However, applying the derivative strategy to bottomhole pressure values monitored downhole could result in smooth pressure derivative profiles.

Investigating different flow regimes in the inverse injectivity plot succeeded for bilinear and radial flow but not for linear flow regime. As anticipated, no linear flow regime was shown because linear fracture flow regime ends early and matrix linear regime appears at late time. On the other hand, radial flow regime was observed in the matrix acidizing case study. The decreasing pressure profile with the unit slope was the indication of the radial flow regime and hence the matrix acidizing.

Calculating fracture area at bilinear flow regime periods showed excellent results. Studying these periods under conditions where the pressure above closure plot indicating no fracture propagation showed good results. First of all, the calculated fracture area was constant during the whole bilinear flow regime, confirming that the constant fracture assumption was right. In addition, the obtained values from both monitoring injection pressure and analyzing data showed great similarity. For the first case, the results were almost identical. Moreover, the fracture area obtained for the second field case was reasonable despite the lack of confirmation of production analysis values. For Well C, the obtained fracture half-length showed similarity to the one obtained from literature for the similar reservoir properties and injection conditions.

The adjustments introduced to Ueda's (2015) work of using the formation fluid properties in calculating the fracture area showed better results compared with the original work. Using different sets of equations depending on the formation type of fluid has been

applied. The use of the conclusion that early data are affected by the formation fluid properties was a key change to the old methodology.

The use of superposition time instead of treatment time has proven to be helpful in calculating the fracture area accurately. As can be seen in the gas wells studied, fracture area increased consistently during the treatment. Treatment time was tested and fluctuating fracture area resulted because of the flow rate variation.

The obtained final fracture area in field cases studied were calculated at periods where non-reactive fluids were injected into the fracture at a high flow rate. As a result, it can be concluded that these values come from the contribution of fracture. In the first case study, the fracture area calculated during the injection of cross-linked acid was less than the values obtained from non-reactive fluids injection periods. This is a proof of the assumption that gelled acid penetrates most of the fracture but not the total area.

To have the most accurate fracture area using the proposed methodology, the following steps can be followed. First, periods in which non-reactive fluids are injected should be analyzed first, and later periods are expected to represent the total fracture area. If all fluids injected are reactive, periods with emulsified acids and gelled acids can be considered, keeping in mind that it is not guaranteed to represent the total area but only most of it. Using this methodology for straight acids and especially with gas wells in carbonate formations results in much underestimated fracture area.

Predicting the general shape of the fracture using Conway's method was helpful. Several factors should be considered to evaluate the general fracture shape beside Conway's method. The events during the treatment, especially at the beginning are helpful

in determining the final shape. Moreover, the formation properties such as the height along with the calculated fracture area can be used to confirm the predicted fracture shape.

The questionable quality of the pressure data observed in case studies where downhole pressure is calculated using surface measured values, especially in the middle of the treatment, can be justified for the following reasons. First of all, the quality of the downhole pressure calculations are not that good because of the successive injection of different fluids with high variation in viscosity. As can be recognized, the quality of data is affected at the middle of the treatment, while good quality is realized at the beginning and end. In addition, the closure pressure value used affects the pressure curve significantly. It would be great if pressure derivative data are smooth and provided to correct the closure pressure value. If not, it is suggested to look for small negative or positive slopes; then the value of closure pressure should be varied to obtain both bounds of PKN and KGD. When the two plots are obtained, the general trend in both scenarios should be analyzed.

In general, the inverse injectivity plot is not affected by the pressure data quality. The main reason is the huge difference between reservoir pressure and bottomhole pressure during injection. On the other hand, the closure pressure is usually close to the injection pressure and a small error in that value can result in a huge difference in results.

Using Bello's method to analyze production data for carbonate tight formation was useful. Although the linear flow regime was not clear, the general linear trend in the normalized pseudo pressure was shown. The simplicity of using that methodology, along

with the accurate results, are encouraging. The introduction of using linear superposition time because of the variable flow rate was successful.

Limitations of the proposed methodology

To analyze the pressure above closure plot with accurate interpretation, it is important that the quality of pressure data and the accuracy of closure pressure is high. Unfortunately, the accuracy of bottomhole pressure calculations is hard to guarantee due to the injection of different fluids that have variations in fluid properties, especially in viscosity. Furthermore, if the derivative pressure data cannot be generated, it is hard to tell whether the closure pressure is accurate or not. However, the general trends and responses of that curve can still be realized and analyzed, as can be seen in the discussed examples in this thesis.

Using derivative pressure data to perform analysis on the data could not be executed in the two discussed stimulated gas wells due to the high sensitivity of derivative data to the pressure data quality. Nevertheless, whenever the quality of pressure data is assured by using downhole gauges for measurements, this curve can be a big help in analyzing fracture propagation.

Calculating the fracture area by analyzing the bilinear flow regime has some limitations. Regarding the model and solution used, fracture permeability is essential for performing calculations which cannot be known in some cases. For the obtained fracture area, it is hard to determine the total fracture area if strong acids are used, the wormholing

effect is not negligible or the permeability and porosity of the formation are high.

However, a minimum fracture area can be confirmed using the calculated fracture area.

CHAPTER IV

CONCLUSIONS AND RECOMMENDATIONS

Conclusions

The major conclusions of my thesis can be summarized as follows:

- 1- Methodologies introduced for hydraulic fracturing treatments to analyze the evolution of the fracture using the pressure above closure and the pressure derivative are applicable in acid fracturing. Pressure derivative analysis needs accurate pressure data to be applicable.
- 2- Combining pressure above closure and inverse injectivity is a very useful tool to understand the treatment progress.
- 3- When the pressure is lower than closure pressure, the fluid cannot penetrate the fracture, radial flow is expected, and matrix acidizing is expected to occur.
- 4- Bilinear flow regime is the dominant flow regime whenever the fracture area is constant and pressure is enough for the fluids to penetrate in the fracture. This flow regime can be tested to estimate the fracture area for oil and gas wells. Etching to the interior walls of the fracture is expected whenever a bilinear flow regime is realized.
- 5- The calculated fracture area can represent either the total fracture area or a portion of the fracture, depending on the type of penetrating fluid and some formation properties.

- 6- Bello's analysis to calculate the fracture area assuming transient linear flow regime in fractured horizontal wells can be applied to carbonate formations.

Recommendations

The following recommendations for future work are listed:

- 1- Investigation of the flow regimes through fractures.
- 2- Introduction of geomechanical properties to help determine more fracture parameters.

REFERENCES

- Ayoub, J. A., Brown, J. E., Barree, R. D., & Elphick, J. J. (1992, February 1). *Diagnosis and Evaluation of Fracturing Treatments*. Society of Petroleum Engineers.
doi:10.2118/20581-PA
- Bazin, B., Roque, C., & Bouteica, M. (1995, January 1). *A Laboratory Evaluation of Acid Propagation in Relation to Acid Fracturing: Results and Interpretation*. Society of Petroleum Engineers. doi:10.2118/30085-MS
- Bello, R. O. (2009). *Rate transient analysis in shale gas reservoirs with transient linear behavior*. Texas A&M University.
- Ben-Naceur, K., & Economides, M. J. (1989, January 1). *Design and Evaluation of Acid Fracturing Treatments*. Society of Petroleum Engineers. doi:10.2118/18978-MS
- Chen, C.-C., & Rajagopal, R. (1997, December 1). *A Multiply-Fractured Horizontal Well in a Rectangular Drainage Region*. Society of Petroleum Engineers.
doi:10.2118/37072-PA
- Chen, C., & Raghavan, R. (2013, January 30). *On Some Characteristic Features of Fractured Horizontal Wells and Conclusions Drawn Thereof*. Society of Petroleum Engineers. doi:10.2118/163104-PA
- Conway, M. W., McGowen, J. M., Gunderson, D. W., & King, D. G. (1985, January 1). *Prediction of Formation Response From Fracture Pressure Behavior*. Society of Petroleum Engineers. doi:10.2118/14263-MS
- Daccord, G. (1987). *Chemical dissolution of a porous medium by a reactive fluid*. Physical Review Letters, 58(5), 479

- Daneshy, A. A. (1973, January 1). *On the Design of Vertical Hydraulic Fractures*. Society of Petroleum Engineers. doi:10.2118/3654-PA
- Economides, M. J., Hill, A. D., Ehlig-Economides, C., & Zhu, D. (2012). *Petroleum production systems*. Pearson Education.
- Geertsma, J., & De Klerk, F. (1969, December 1). *A Rapid Method of Predicting Width and Extent of Hydraulically Induced Fractures*. Society of Petroleum Engineers. doi:10.2118/2458-PA
- Guo, F., Morgenstern, N. R., & Scott, J. D. (1994, June 1). *Interpretation And Analysis of Hydraulic Fracture Pressures*. Petroleum Society of Canada. doi:10.2118/94-06-01
- Hill, A. D., & Zhu, D. (1996, May 1). *Real-Time Monitoring of Matrix Acidizing Including the Effects of Diverting Agents*. Society of Petroleum Engineers. doi:10.2118/28548-PA
- Hill, A. D., Zhu, D., & Wang, Y. (1995, November 1). *The Effect of Wormholing on the Fluid Loss Coefficient in Acid Fracturing*. Society of Petroleum Engineers. doi:10.2118/27403-PA
- Kalfayan, L. (2008). *Production enhancement with acid stimulation*. Pennwell Books
- Kim, G. H., & Wang, J. Y. (2011, January 1). *Interpretation of Hydraulic Fracturing Pressure in Low-Permeability Gas Formations*. Society of Petroleum Engineers. doi:10.2118/141525-MS
- Larsen, L., & Bratvold, R. B. (1994, June 1). *Effects of Propagating Fractures on Pressure-Transient Injection and Falloff Data*. Society of Petroleum Engineers.

doi:10.2118/20580-PA

Liu, G., & Ehlig-Economides, C. (2015, September 28). *Comprehensive Global Model for Before-Closure Analysis of an Injection Falloff Fracture Calibration Test*.

Society of Petroleum Engineers. doi:10.2118/174906-MS

Medeiros, F., Ozkan, E., & Kazemi, H. (2008, October 1). *Productivity and Drainage Area of Fractured Horizontal Wells in Tight Gas Reservoirs*. Society of

Petroleum Engineers. doi:10.2118/108110-PA

Nolte, K. G. (1988, January 1). *Fluid Flow Considerations in Hydraulic Fracturing*.

Society of Petroleum Engineers. doi:10.2118/18537-MS

Nolte, K. G. (1988, February 1). *Principles for Fracture Design Based on Pressure Analysis*. Society of Petroleum Engineers. doi:10.2118/10911-PA

Nolte, K. G. (1991, February 1). *Fracturing-Pressure Analysis for Nonideal Behavior*.

Society of Petroleum Engineers. doi:10.2118/20704-PA

Nolte, K. G., & Smith, M. B. (1981, September 1). *Interpretation of Fracturing*

Pressures. Society of Petroleum Engineers. doi:10.2118/8297-PA

Nordgren, R. P. (1972, August 1). *Propagation of a Vertical Hydraulic Fracture*.

Society of Petroleum Engineers. doi:10.2118/3009-PA

Perkins, T. K., & Kern, L. R. (1961, September 1). *Widths of Hydraulic Fractures*.

Society of Petroleum Engineers. doi:10.2118/89-PA

Rosolen, M. A. (1997, January 1). *Pressure Analysis on Hydraulic Fracturing*. Society of Petroleum Engineers. doi:10.2118/38954-MS

Ueda, K., Zhang, W., Zhu, D., Hill, A. D., Zhang, F., & Yang, X. (2016, February 1).

Evaluation of Acid Fracturing by Integrated Pressure Analysis and 3D

Simulation: A Field Application for Multi-Stage Stimulation in Horizontal Wells.

Society of Petroleum Engineers. doi:10.2118/179123-MS

Ueda, K. (2015). *Integrated method to evaluate acid stimulation of horizontal wells in carbonate reservoir through treatment pressure analysis.* Texas A&M University.